IOPscience iopscience.iop.org

Home Search Collections Journals About Contact us My IOPscience

Galerkin method for feedback controlled Rayleigh–Bénard convection

This article has been downloaded from IOPscience. Please scroll down to see the full text article.

2008 Nonlinearity 21 2625

(http://iopscience.iop.org/0951-7715/21/11/008)

View the table of contents for this issue, or go to the journal homepage for more

Download details:
IP Address: 129.67.186.247
The article was downloaded on 13/11/2011 at 22:29

Please note that terms and conditions apply.

IOP PUBLISHING NONLINEARITY

Nonlinearity **21** (2008) 2625–2651 doi:10.1088/0951-7715/21/11/008

Galerkin method for feedback controlled Rayleigh–Bénard convection*

A Münch[1] **and B Wagner**[2]

[1] Theoretical Mechanics Section, School of Mathematical Sciences, University of Nottingham, Nottingham NG7 2RD, UK
[2] Weierstrass Institute for Applied Analysis and Stochastics (WIAS), Mohrenstr. 39, 10117 Berlin, Germany

E-mail: andreas.muench@nottingham.ac.uk and wagnerb@wias-berlin.de

Received 20 July 2007, in final form 8 August 2008
Published 10 October 2008
Online at stacks.iop.org/Non/21/2625

Recommended by A L Bertozzi

Abstract

The problem of feedback controlled Rayleigh–Bénard convection is considered. For this problem with the simple flow structure in the vertical direction, a Galerkin method that uses only a few basis functions in this direction is presented. This approximation yields considerable simplification of the problem, explicitly incorporates the non-classical boundary conditions at the horizontal boundaries of the fluid layer resulting from feedback control and reduces the dimension of the original problem by one. This method is in spirit very similar to lubrication theory, where the simple laminar flow in the vertical direction is integrated out across the height of the fluid layer.

Using a minimal set of appropriate basis functions to capture the nonlinear behaviour of the flow, we investigate the effects of feedback control on amplitude, wavelength and selection of patterns via weakly nonlinear analysis and numerical simulations of the resulting dimension-reduced problems in two and three dimensions.

In the second part of this study we discuss the derivation of the appropriate basis functions and prove convergence of the Galerkin scheme.

Mathematics Subject Classification: 74D10, 74F05, 74F10, 77N25

PACS numbers: 68.15.+e

(Some figures in this article are in colour only in the electronic version)

* This paper is published as part of a collection in honour of Todd Dupont's 65th birthday.

 © 2008 IOP Publishing Ltd and London Mathematical Society Printed in the UK

1. Introduction

Rayleigh–Bénard convection occurs abundantly in nature, such as in oceans and the atmosphere, as well as in many technological processes, wherever heat transport or fluid mixing becomes relevant. Since the pioneering works by Lord Rayleigh [1] and Bénard [2], numerous experimental and theoretical studies have been undertaken, in part because of the relative ease of producing accurate experimental data and on the other hand because of the rich dynamical behaviour of the Rayleigh–Bénard system, which plays a fundamental role in the theory of pattern forming systems. Apart from some of the earliest theoretical studies by Busse [3, 4] we refer here to [5] and more specifically [6] and [7] for a review and many references therein.

In the most basic experimental setting Rayleigh–Bénard convection arises when a quiescent fluid layer inside a closed container is heated from below. Above a certain vertical temperature difference, quantified by the Rayleigh number (Ra), buoyancy forces destabilize the fluid leading to the appearance of rolls and more complicated patterns as the temperature difference is increased. Experimental investigations of large-aspect-ratio Rayleigh–Bénard systems have led to the discovery of further instabilities, and for example the appearance of spiral-defect chaos [8–11]. Apart from the aspect ratio and boundary effects from the side walls, these instabilities also depend on the value of the Prandtl number (Pr) and, for the case of spiral-defect chaos, they even occur for parameter values where straight convection rolls are stable. Theoretical work is typically based on the one hand on the Boussinesq equation [12, 13] and on the other hand on model equations such as the Swift–Hohenberg model [14–16] and generalizations thereof. One disadvantage of the Swift–Hohenberg models is that there is no rigorous derivation from the underlying Boussinesq equations and moreover for spiral-defect chaos these models may predict incorrect behaviour [17].

Apart from the scientific interest, for many technological applications it is important to investigate the feasibility of controlling and modifying the arising patterns such as described above. A typical example is Czochralski crystal growth [18], where during the growth process convection in the melt may cause inhomogeneities of dopants. Here, suppression or delay of onset of the instability is desirable. With respect to this objective it is desirable to explore the potential of active feedback control and develop mathematical models and methods that allow for an efficient treatment of the control problems at hand.

Experimentally, various strategies have been pursued in a series of works by Tang and Bau [19–21] as well as by Howle [22–24], and more recently followed up by [25–28], where the onset of convection could be delayed by several factors of the critical Rayleigh number. The basic strategy, as pursued originally by Tang and Bau, is to cancel convection in the Rayleigh–Bénard system by imposing a temperature distribution at the lower boundary in proportion to a measured temperature distribution in the middle of the fluid layer. Alternatively, control via an imposed velocity distribution at the lower boundary was investigated. A different strategy is pursued by Howle. Here, the heat flux at the lower boundary is used as a feedback control, since prescribing the heat flux is experimentally easier. On the upper boundary an uniform temperature is imposed and the velocity obeys the no-slip conditions on the upper and lower boundaries. The control law specifies the spatial distribution of the heat flux on the lower boundary while keeping the spatial mean heat flux constant. In this way the control of the heat flux acts so as to aid the natural dissipation in the system and as a consequence negative feedback control delays the onset of convection.

In Howle's experiments the wave pattern is obtained by shadowgraphic visualization of the state of the system. In order to use this as an input for the control law an expression for the shadowgraphic wave pattern, originally derived in [29], is used in the derivation of the condition

at the lower boundary. The active feedback control then sets the heat flux at the lower boundary proportional to the shadowgraphic signal. In [30] comparison of the experimental results with predictions of linear stability analysis of the negative feedback-controlled Boussinesq equations shows good agreement. In [31] it was shown theoretically that positive feedback control of the Boussinesq equation may lead to an ill-posed problem, which is removed by an extension of the model that includes more details of the control boundary, such as the thickness of the boundary. It is then shown that not only for negative but also for positive feedback control the delay or advance of the onset of the instability remains bounded as the strength of the control parameter is increased.

Via a mathematical model for this control mechanism, we will here also answer questions on the change in amplitude at the new critical conditions as the strength of the feedback control is varied and in higher dimensions investigate the impact on pattern selection. A goal of practical interest would certainly be to directly modify fluid patterns.

The contribution we intend to make in this direction is threefold:

First, we make use of the property that while the convection patterns may have a complicated structure in the horizontal large-scale directions, the flow field and the temperature distribution in the small-scale vertical direction are simple for the large-aspect ratios considered in the experiments we discussed above.

In this case it is very convenient to use dimension-reduced models derived from the underlying Boussinesq equation via a Galerkin approximation to efficiently explore the bifurcation structure of the control problem. The objective of the Galerkin approximation discussed here is to represent the flow variables by a linear combination of basis functions, using a small number (one or two) of low degree polynomials for the vertical direction, such that the boundary conditions are explicitly satisfied. Essentially it is a projection method that projects an approximate structure of the solution together with the original problem onto a space of basis functions, within which the approximated problem is solved. In this way the number of spatial dimensions of the boundary value problem is reduced by one. This approximation can be systematically derived from the underlying governing equations, here the Boussinesq equations, it is easily extendable to include higher order structures by allowing for more basis functions and its accuracy can be determined.

We note that it is similar in spirit to the lubrication approximation. There, one explicitly uses the length-scale separation to reduce the Navier–Stokes equations and then integrates out the dependence of the laminar flow in the vertical direction. Here, one has to incorporate a small number of basis functions to account for the simple flow structure in one direction and upon integrating that out, to obtain a dimension-reduced problem.

We point out that the underlying idea of the Galerkin approximation is a generic concept and similar approximations have also been developed by other groups. Most notably, the group around Pesch [12, 13] and Busse [4] who applied it to a number of problems related to Rayleigh–Bénard convection such as for example convection in liquid crystals [32]. Furthermore, Manneville and coworkers used a similar Galerkin approximation in the context of Rayleigh–Bénard convection in [33] and more recently also for other problems, such as for plane Couette flow [34] and for flow down an inclined plane [35].

The derivation used in this study was originally inspired by [36]. They applied their approach to a variety of problems, including Rayleigh–Bénard convection in 2D, formation of shocks in suspensions or colloids. Their approach has been extended further to the Rayleigh–Bénard problem that includes non-classical boundary conditions resulting from feedback control in [31]. Here, we go beyond linear analysis for the reduced models and furthermore extend the approximation to three dimensions.

Second, the Galerkin method discussed in these studies is well suited to include complicated boundary conditions allowing us to use realistic and experimentally tested feedback control mechanisms into our model and the perspective to compare with experimental results.

Third, we prove convergence of the approximation method.

In the following section we formulate the feedback controlled Rayleigh–Bénard problem and derive dimension-reduced models for one and two basis functions. In section 3 we perform a weakly nonlinear stability analysis. In section 4 we extend the derivation to three dimensions and investigate numerically the patterns selected by applying feedback control. In section 5 we address the peculiarities of artificial singularities as they appear for positive feedback control. We observe that this already occurs for the central problem of the feedback controlled heat equation. We derive appropriate conditions for the basis function to resolve this problem and finally prove convergence of the resulting Galerkin scheme. We conclude with a short discussion on spiral-defect chaos, derive the corresponding Galerkin approximation and show some numerical results.

2. Formulation

The governing equations for the convection layer are the Boussinesq equation together with the continuity and energy equations. In dimensionless form they are

$$Pr^{-1}[\partial_t \boldsymbol{u} + (\boldsymbol{u}\cdot\boldsymbol{\nabla})\boldsymbol{u}] = -\boldsymbol{\nabla} p + R\ T^+\ (0,0,1)^t + \nabla^2 \boldsymbol{u}, \tag{2.1}$$

$$\boldsymbol{\nabla}\cdot\boldsymbol{u} = 0, \tag{2.2}$$

$$\partial_t T + \boldsymbol{u}\cdot\boldsymbol{\nabla} T = \nabla^2 T + w, \tag{2.3}$$

where the scalings

$$\left.\begin{aligned} &(x,y,z) = \left(\frac{x^*}{d}, \frac{y^*}{d}, \frac{z^*}{d}\right), \qquad t = \frac{\kappa}{d^2}t^*, \qquad (u,v,w) = \frac{d}{\kappa}(u^*, v^*, w^*), \\ &T^+ = \frac{k}{\bar{q}d}T^*, \qquad p = \frac{d^2}{\rho\kappa^2}p^*. \end{aligned}\right\} \tag{2.4}$$

have been used. We denote by d, κ, ρ and $\bar{q}$ the height of the fluid layer, thermal diffusivity, fluid density and spatially averaged heat flux, respectively. We further write

$$\boldsymbol{u} = (u,v,w), \qquad T^+ = T_c + T = \theta_u - \left(z - \frac{1}{2}\right) + T \tag{2.5}$$

with the conductive state T_c and the temperature θ_u on the upper boundary $z = 1/2$.

$$R = \frac{g\alpha\bar{q}d^4}{\kappa\nu k_{\mathrm{th}}} \qquad \text{and} \qquad Pr = \frac{\nu}{\kappa} \tag{2.6}$$

denote the Rayleigh and the Prandtl number, with k_{th}, α, g and ν the thermal conductivity, thermal expansion coefficient, gravity and viscosity, respectively. Except for the treatment of the spiral-defect chaos we assume the Prandtl number to be large and therefore neglect the left-hand side of (2.1). This is in accordance with the experimental situation of [22].

We assume solutions are periodic in x and y and satisfy no-slip and no-penetration conditions at the upper and lower boundaries

$$u = v = w = 0 \qquad \text{at } z = \pm\tfrac{1}{2}. \tag{2.7}$$

In experiments by [24] the temperature is kept fixed at the upper boundary. Hence, we have

$$T = 0 \qquad \text{at } z = +\tfrac{1}{2}. \tag{2.8}$$

The feedback control boundary condition at the lower boundary is derived as follows. The spatial distribution of the heat flux q at the lower boundary is set proportional to the shadowgraphic signal. In addition the heat flux is also set proportional to the time derivative of the shadowgraphic signal in [23], but we will neglect this contribution here. The heat flux $q = -k_{\mathrm{th}}\partial_z T$ is then given by

$$q = \bar{q}\left(1 + c\frac{\delta I(\boldsymbol{x})}{I_0}\right), \tag{2.9}$$

where c is a proportionality factor of the shadowgraphic signal $\delta I(\boldsymbol{x})/I_0$, I_0 being the uniform brightness at reference state. An expression for the shadowgraphic signal in terms of the temperature was derived in [29] and is given by

$$\frac{\delta I(\boldsymbol{x})}{I_0} = -2H\frac{\mathrm{d}\eta}{\mathrm{d}T}\,\Delta_2\int_{-d/2}^{d/2} T\,\mathrm{d}z \tag{2.10}$$

as long as the ratio of the height of the fluid layer d over the distance of the fluid layer to the image plane H is large. Here, η denotes the refractive index, which usually decreases as the temperature increases, i.e. $\mathrm{d}\eta/\mathrm{d}T$ is negative. Hence the dimensionless expression for T in (2.5) is

$$\partial_z T = -\omega\,\Delta_2\int_{-1/2}^{1/2} T\,\mathrm{d}z \qquad \text{at } z = -\frac{1}{2}, \tag{2.11}$$

where $\Delta_2 = \partial_x^2 + \partial_y^2$ and the dimensionless proportionality factor

$$\omega = \frac{2cH}{d}\left(-\frac{\mathrm{d}\eta}{\mathrm{d}T}\right) \tag{2.12}$$

is the control parameter. Hence for positive c (i.e. negative feedback control), $\omega > 0$. Moreover, the integral of the shadowgraphic signal over x and y is zero, so that the global Rayleigh number is not altered by the control.

In [31] it was also found that the problem may become ill posed for $\omega < -1$, i.e. for a critical positive proportionality factor. This is readily understood for the much simpler linear problem for the heat equation $\partial_t T = \Delta T$ with control boundary condition (2.11) at $z = -1/2$ and no-flux boundary condition $\partial_z T = 0$ on the upper boundary $z = 1/2$. Integrating the heat equation from $z = -1/2$ to $z = 1/2$ and taking the Fourier transform of the result in the lateral directions gives

$$\partial_t \hat{T}(k,t) = -(\omega+1)k^2\hat{T}(k,t), \qquad \text{where } \hat{T}(k,t) = \int_{-1/2}^{1/2}\int \mathrm{e}^{-\mathrm{i}kz}T(x,z,t)\,\mathrm{d}x\,\mathrm{d}z,$$

given here in two dimensions for simplicity. It is now easily seen that the one-dimensional spectrum decays like a diffusion process with $-(\omega+1)$ as the diffusion coefficient. Clearly, $\omega < -1$ yields a diffusion process which is backward in time and renders the problem ill-posed in the sense that perturbations at high wave number k are amplified at a rate proportional to k^2. This and the extension of this argument to positive feedback-controlled Rayleigh–Bénard convection is given in detail in [31], as well as the treatment of the extended model that takes into account boundary properties such as boundary thickness or heater size.

2.1. Galerkin method

We first briefly present the derivation of the dimension-reduced problem in 2D for simplicity, see also [31]. We begin by representing the flow variables by a linear combination of basis functions, using only a small number of low degree polynomials for the z-direction. By testing

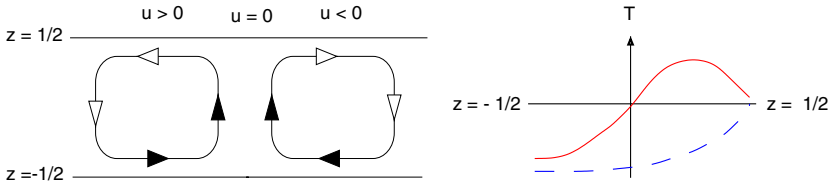

Figure 1. Streamlines for (2.13)–(2.14) (left). Polynomials for the temperature $H_0(z)$ (dashed) and $H_1(z)$ (solid).

with the basis functions (i.e. multiplying by the basis functions and integrating over the domain) each equation of the governing system is replaced by a small number of equations of lower dimension. The usefulness of this method is due to the fact that in many cases the patterns that arise in hydrodynamic instabilities can be approximated by one or two polynomials.

Within the context of Rayleigh–Bénard convection the idea to use a Galerkin projection method to eliminate the vertical dependence and obtain reduced model equations has also been used by Manneville [33] using a basis of eigenmodes of the linearized problem. His exposition includes some discussion of the dimension-reduced partial differential equations and a comparison with alternative approximations using amplitude equations. A few-mode Galerkin technique was also frequently applied by Pesch and collaborators, see for example [12], where they use Chandresekhar functions for their numerical computations.

In our approach we first need to determine the minimal number of polynomials necessary to capture the dominant nonlinearity. The minimal polynomial representation for the velocity components (v, w) that satisfy the no-slip boundary and non-permeability conditions at $z = \pm 1/2$ and the continuity equation is

$$v(x, z, t) = u(x, t)\, \mu_z(z), \qquad w(x, z, t) = -u_x(x, t)\mu(z), \tag{2.13}$$

where

$$\mu(z) = \frac{1}{4}\left(z^2 - \frac{1}{4}\right)^2. \tag{2.14}$$

Figure 1 shows streamlines of a roll pattern produced by (2.13)–(2.14) for periodic $u(x, t)$. Note that $u(x, t)$ is not to be confused with the 3D horizontal velocity $u(x, y, z, t)$.

The temperature satisfies a non-homogeneous boundary condition with feedback control. We take this into account by making the following ansatz for the Galerkin approximation of the temperature field:

$$T(x, z, t) = h(x, t)\, H_0(z) + s(x, t)\, \ell(z), \tag{2.15}$$

where we have split the temperature into a contribution for the problem with homogeneous boundary conditions plus a term that models the control boundary conditions. This means that

$$H_0(1/2) = 0 \qquad \text{and} \qquad H_0'(-1/2) = 0, \tag{2.16}$$

$$\ell(1/2) = 0 \qquad \text{and} \qquad \ell'(-1/2) = 1. \tag{2.17}$$

The lowest order polynomial $H_0(z)$ that satisfies the conditions (2.16) is

$$H_0(z) = \left(z - \frac{1}{2}\right)\left(z + \frac{3}{2}\right), \tag{2.18}$$

see the dashed curve in figure 1. This representation of the temperature is capable of producing temperature fields which are not symmetric with respect to zero.

This is not so, if for example we had chosen Neumann boundary conditions on both sides, see [36]. In this case we would have needed a third order polynomial as well in order to break the symmetry of the temperature profile.

In section 5 we show that the polynomial $\ell(z)$ not only needs to satisfy conditions (2.17) but also in order to prevent artificial singularities that arise through this approximation, for positive feedback control, we need to require

$$\rho_1 = \int_{-1/2}^{1/2} \ell(z)\,\mathrm{d}z = \langle \ell, H_0 \rangle \int_{-1/2}^{1/2} H_0(z)\,\mathrm{d}z \tag{2.19}$$

with

$$\langle \ell, H_0 \rangle = \int_{-1/2}^{1/2} \ell(z) H_0(z)\,\mathrm{d}z. \tag{2.20}$$

We give a derivation of this in section 5. In order to simplify calculations we choose $\ell(z)$ to be orthogonal to $H_0(z)$, i.e. the scalar product $\langle \ell, H_0 \rangle = 0$, and therefore also $\rho_1 = 0$. This leads us to the polynomial

$$\ell(z) = \left(z - \frac{1}{2}\right)\left(z^2 + \frac{1}{8}z - \frac{1}{16}\right). \tag{2.21}$$

We obtain the Galerkin approximation by testing the full problem with the functions

$$\theta_0 = \delta(x)\,\mu_z(z), \qquad \theta_1 = -\delta'(x)\,\mu_z(z), \qquad \phi_0 = \delta(x) H_0(z), \tag{2.22}$$

to obtain

$$\partial_x^4 u - 24\,\partial_x^2 u + 504\,u = -R\;\partial_x\left(60\,h - \frac{3}{2}\,s\right), \tag{2.23}$$

$$\begin{aligned}\partial_t h - \partial_x^2 h + \frac{5}{2}h + \frac{9}{448}\left(u\partial_x h + \frac{1}{2}h\partial_x u\right)\\ = \frac{15}{8}s + \frac{5}{448}\partial_x u + \frac{u\partial_x s - 3/2\,s\,\partial_x u}{448\cdot 24}.\end{aligned} \tag{2.24}$$

Finally, introducing (2.15) and (2.21) into the control boundary condition (2.11) yields

$$s = \omega\tfrac{2}{3}\partial_x^2 h. \tag{2.25}$$

The system of partial differential equations are not only much easier to treat numerically because of the reduced dimension, but, as we will see in the following section, its analytical treatment is much simpler.

3. Weakly nonlinear stability

We first recall from [31] that for this Galerkin approximation, linearization about the conductive state $h(x,t) = 0$, $u(x,t) = 0$, reduces the linear stability problem to solving

$$\partial_t \hat{h} = \sigma(k,\omega)\hat{h} \tag{3.1}$$

with growth rate

$$\sigma(k,\omega) = -\left(k^2 + \frac{5}{2}\right) + \frac{75}{112}MR + \omega k^2\left(\frac{5}{448}MR - \frac{5}{4}\right). \tag{3.2}$$

$\hat{h}(k,t)$ denotes the Fourier transform of $h(x,t)$ and

$$M = \frac{k^2}{k^4 + 24\,k^2 + 504}, \tag{3.3}$$

which yields the critical Rayleigh number as a function of the feedback control parameter,

$$R_c(\omega) = \frac{28}{15}\frac{(4+5\omega)\left(k_c^4+24k_c^2+504\right)^2}{(2\omega-5)\,k_c^4+84\omega k_c^2+2520}, \tag{3.4}$$

where $k_c(\omega)$ is the solution of the polynomial

$$(4+5\omega)(\omega k^8+120k^6)+(6360+4944\omega-2520\omega^2)k^4 \tag{3.5}$$

$$-10080\omega k^2-302400=0. \tag{3.6}$$

The approximation yields rather good results, even though only one basis function has been used. For example when $\omega = 0$ (uncontrolled Rayleigh–Bénard convection with rigid boundaries and Dirichlet/Neumann conditions for the temperature) we have $R_c = 1446$ and $k_c = 2.39$ for the reduced model (with one basis function for the temperature) compared with $R_c = 1296$ and $k_c = 2.55$ for the full Boussinesq equations (2.1)–(2.11), which is a difference of about 12% and 6%, respectively. The accuracy can be easily improved by using more basis functions. For example, if we use a two-function model, which is the reduced model obtain by the Galerkin method using two basis functions for the temperature (instead of one), then we obtain $R_c = 1350$ and $k_c = 2.52$. This is a difference of just 4% and 1%, respectively. The reduced model for two basis functions and the linear stability analysis for it is included in appendix A.2.

The nonlinear behaviour near R_c is described by the Landau equations for the amplitude. Their derivation from the original governing equations is often problematic if the boundary conditions are other than Neumann conditions. The Galerkin approximation removes boundaries in the z-direction. We show how the Landau equation for feedback controlled Rayleigh–Bénard convection can be derived on the basis of multiple-scale asymptotics.

Suppose the system experiences a small initial perturbation

$$\boldsymbol{w}(x,0) = \delta(\bar{u}(x),\bar{h}(x)), \qquad \boldsymbol{w}=(u,h), \tag{3.7}$$

where $\delta \ll 1$. When we rescale the problem by δ as

$$u = \delta u^*, \qquad h = \delta h^*, \tag{3.8}$$

drop the $*$ and denote

$$\mathcal{L}_u(\boldsymbol{w}) := \partial_x^4 u - 24\,\partial_x^2 u + 504\,u + R\;\partial_x\left(60\,h-\frac{3}{2}\,s\right), \tag{3.9}$$

$$\mathcal{L}_h(\boldsymbol{w}) := \partial_t h - \partial_x^2 h + \frac{5}{2}h - \frac{15}{8}s - \frac{5}{448}\partial_x u, \tag{3.10}$$

then, in the scaled problem, the nonlinear terms appear as a small correction:

$$\mathcal{L}_u(\boldsymbol{w}) = 0, \tag{3.11}$$

$$\mathcal{L}_h(\boldsymbol{w}) = \frac{\delta}{448}\left[-9\left(u\partial_x h+\frac{1}{2}h\partial_x u\right)+\frac{\omega}{24}\left(\frac{2}{3}u\partial_{xxx}h-\partial_{xx}h\partial_x u\right)\right]. \tag{3.12}$$

In the x-direction we assume periodic boundary conditions. For this perturbation problem we make the ansatz

$$\boldsymbol{w}(x,t;\delta) := \boldsymbol{w}_0(x,t,\tau)+\delta\boldsymbol{w}_1(x,t,\tau)+\delta^2\boldsymbol{w}_2(x,t,\tau)+O(\delta^3), \tag{3.13}$$

$$R = R_c+\delta^2\alpha, \qquad \tau = \delta^2 t. \tag{3.14}$$

To leading order we basically get the linear stability problem

$$\mathcal{L}_u(\boldsymbol{w}_0) = 0, \quad \mathcal{L}_h(\boldsymbol{w}_0) = 0, \tag{3.15}$$

$$\text{with initial conditions: } \boldsymbol{w}_0(x,0) = (\bar{u}(x),\ \bar{h}(x)). \tag{3.16}$$

To O(δ) we get

$$\mathcal{L}_u(\boldsymbol{w}_1) = 0, \tag{3.17}$$

$$\mathcal{L}_h(\boldsymbol{w}_1) = \frac{1}{448}\left(-9\left[u_0\partial_x h_0 + \frac{1}{2}h_0\partial_x u_0\right] + \frac{\omega}{24}\left[\frac{2}{3}u_0\partial_{xxx}h_0 - \partial_{xx}h_0\partial_x u_0\right]\right). \tag{3.18}$$

To O(δ^2) we find

$$\mathcal{L}_u(\boldsymbol{w}_2) = -\alpha\ (60\,\partial_x h_0 - \omega\partial_{xxx}h_0)\,, \tag{3.19}$$

$$\begin{aligned}\mathcal{L}_h(\boldsymbol{w}_2) = &-\partial_\tau h_0 - \frac{9}{448}\left(u_1\partial_x h_0 + u_0\partial_x h_1 + \frac{1}{2}\left(h_0\partial_x u_1 + h_1\partial_x u_0\right)\right)\\ &+ \frac{\omega}{448\cdot 24}\left(\frac{2}{3}u_0\partial_{xxx}h_1 + \frac{2}{3}u_1\partial_{xxx}h_0 - \partial_{xx}h_0\partial_x u_1 - \partial_{xx}h_1\partial_x u_0\right).\end{aligned} \tag{3.20}$$

Since we have periodic boundary conditions the solution can be written in the form

$$h_0(x,t,\tau) = \sum_{n=1}^{\infty} A_n(t,\tau)\sin(nk_c x) + B_n(t,\tau)\cos(nk_c x), \tag{3.21}$$

$$u_0(x,t,\tau) = \sum_{n=1}^{\infty} E_n(t,\tau)\sin(nk_c x) + F_n(t,\tau)\cos(nk_c x), \tag{3.22}$$

with

$$A_n(t,\tau) = K(\tau)\mathrm{e}^{\sigma_n t}, \qquad B_n(t,\tau) = L(\tau)\mathrm{e}^{\sigma_n t}$$

$$E_n(t,\tau) = V_n A_n(t,\tau), \qquad F_n(t,\tau) = -V_n B_n(t,\tau),$$

$$V_n = \frac{R_c M_n}{nk_c}\left(60 + \omega(k_c n)^2\right), \qquad M_n = \frac{(nk_c)^2}{(nk_c)^4 + 24(nk_c)^2 + 504},$$

$$\sigma_n = -\left((nk_c)^2 + \frac{5}{2}\right) + \frac{75}{112}M_n R_c + \omega(k_c n)^2\left(\frac{5}{448}M_n R_c - \frac{5}{4}\right).$$

The leading order solution corresponds to the solution to the linear stability problem at criticality. This means that there $\sigma_1 = 0$, while for all other σ_{in} we have $\mathrm{Re}(\sigma_{in}) < 0$. Hence, the dominant terms in the expansions are

$$h_0 = K(\tau)\sin(k_c x) + L(\tau)\cos(k_c x), \qquad u_0 = V_1\left[L(\tau)\sin(k_c x) - K(\tau)\cos(k_c x)\right] \tag{3.23}$$

while all other terms decay.

The unknown functions $K(\tau)$ and $L(\tau)$ have to be determined by solving the higher order problems. To O(δ) we obtain the solution

$$h_1 = \rho_1(K^2 + L^2) + \rho_2\left[(L^2 - K^2)\cos(2k_c x) - 2KL\sin(2k_c x)\right], \tag{3.24}$$

$$u_1 = q_1\left[(L^2 - K^2)\sin(2k_c x) - 2KL\cos(2k_c x)\right], \tag{3.25}$$

where

$$\rho_1 = \frac{V_1 k_c}{448}\left(\frac{9}{10} + \omega\frac{k_c^2}{72}\right), \qquad \rho_2 = \frac{V_1 k_c}{448\sigma_2}\left(\frac{27}{4} + \omega\frac{k_c^2}{144}\right),$$

$$q_1 = \frac{1}{448}\frac{V_1 V_2 k_c}{\sigma_2}\left(\frac{27}{4} - \omega\frac{k_c^2}{144}\right).$$

Note that the right-hand side of (3.19)–(3.20) contains linear combinations of $\sin(k_c x)$, $\cos(k_c x)$ etc. Hence, we make the following ansatz for the solution to u_2 and h_2:

$$u_2 = \mu_1(\tau)\sin(k_c x) + \nu_1(\tau)\cos(k_c x), \qquad h_2 = \mu_2(\tau)\sin(k_c x) + \nu_2(\tau)\cos(k_c x). \tag{3.26}$$

If we now sort both sides of the $O(\delta^2)$ equation with respect to $\sin(k_c x)$ and $\cos(k_c x)$ we obtain four equations for the unknowns μ_1, ν_1, μ_2, ν_2. In vector notation this reads

$$\begin{pmatrix} 1 & 0 & 0 & -R_c M_1 \zeta \\ 0 & 1 & R_c M_1 \zeta & 0 \\ 0 & 0 & \sigma_1 & 0 \\ 0 & 0 & 0 & \sigma_1 \end{pmatrix} \begin{pmatrix} \mu_1 \\ \nu_1 \\ \mu_2 \\ \nu_2 \end{pmatrix} = \begin{pmatrix} \alpha L \zeta \\ -\alpha K \zeta \\ \text{Equation for } K \\ \text{Equation for } L \end{pmatrix}, \tag{3.27}$$

where

$$\zeta = \frac{M_1\left(60 + \omega k_c^2\right)}{k_c(\omega)} \qquad \text{and} \qquad \sigma_1 = \sigma_1\left(k_c(\omega), R_c(\omega)\right).$$

Note that $\sigma_1(k_c(\omega), R_c(\omega)) = 0$. Therefore, the solvability condition requires that the equation for K and the equation for L on the right-hand side are zero:

$$\frac{\mathrm{d}K}{\mathrm{d}\tau} - a(\alpha,\omega)\,K - b(\omega)\,K\,(K^2 + L^2) = 0, \tag{3.28}$$

$$\frac{\mathrm{d}L}{\mathrm{d}\tau} - a(\alpha,\omega)\,L - b(\omega)\,L\,(K^2 + L^2) = 0, \tag{3.29}$$

where

$$a(\alpha,\omega) = \frac{5}{448}\alpha M_1(60 + \omega k_c^2),$$

$$b(\omega) = \frac{k_c}{448}\left[9V_1\left(\rho_1 - \frac{1}{2}\rho_2\right) - \frac{\omega k_c^2}{24}\left(\frac{4}{3}q_1 + \frac{14}{3}\rho_2 V_1\right)\right].$$

These are often also called the Landau equations. From linear theory we note that

$$\mathrm{sgn}(a) = \mathrm{sgn}(\alpha) = \mathrm{sgn}(R - R_c)$$

and that $b(\omega) > 0$, so that we always have a supercritical bifurcation for any ω. We find that feedback control decreases amplitudes if feedback control is positive, while they are increased for negative feedback control. This is illustrated in figure 2 for the u-amplitudes for $\omega = -0.9, -0.4, 0.4, 0.9$. On the right of figure 2 we compare the results of the weakly nonlinear analysis to the numerical solution of the Galerkin model for $\omega = -0.4$ for the h-amplitude.

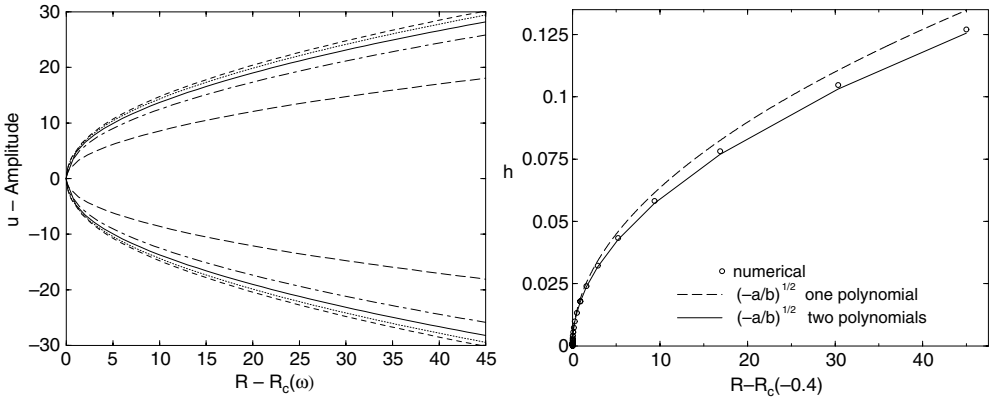

Figure 2. Amplitude for u using the Galerkin approximation with two temperature function (left). Comparison of the amplitude for the temperature using weakly nonlinear results from the Galerkin approximation with one and two temperature function (right)

4. Pattern selection for 3D feedback controlled Rayleigh–Bénard convection

In 3D we observe that any divergence free velocity field in the domain $-1/2 < z < 1/2$ can be written as the curl of a vector field

$$\boldsymbol{u} = \langle u, v, w\rangle = \boldsymbol{\nabla} \times \boldsymbol{B} \qquad \text{with } \boldsymbol{B} = \langle \phi, \varphi, 0\rangle. \tag{4.1}$$

Taking the curl of (2.1) and noting that $Pr^{-1} \ll 1$ we obtain for (2.1)

$$\left\langle \begin{matrix} -\Delta^2\phi + \Delta\left(\partial_x^2\phi + \partial_y\partial_x\varphi\right) + R\,\partial_y T \\ -\Delta^2\varphi + \Delta\left(\partial_x\partial_y\phi + \partial_y^2\varphi\right) - R\,\partial_x T \\ \Delta\left(\partial_x\partial_z\phi + \partial_y\partial_z\varphi\right) \end{matrix} \right\rangle = 0. \tag{4.2}$$

We now seek a minimal polynomial representation for the components of $\boldsymbol{B}$

$$\phi = U(x, y, t)\,\mu(z), \qquad \varphi = V(x, y, t)\,\mu(z), \tag{4.3}$$

that enables us to capture the three-dimensional convection cell pattern. In particular, the components of $\boldsymbol{u}$,

$$u = \mu\,\partial_y W - V\,\partial_z\mu, \qquad v = -\mu\,\partial_x W + U\,\partial_z\mu, \qquad w = \mu\,\partial_x V - \mu\,\partial_y U, \tag{4.4}$$

must satisfy the boundary conditions at $z = \pm 1/2$. The polynomial of minimal degree that meets this requirement is again $\mu(z) = 1/4(z^2 - 1/4)^2$. Note also that by letting $U = 0$, $V = -u(x, t)$ in (4.4), we recover our previous ansatz (2.13) for the case of two-dimensional Rayleigh–Bénard convection.

For the temperature we make analogously to the two-dimensional case the ansatz

$$T = h(x, y, t)\,H(z) + s(x, y, t)\,\ell(z), \tag{4.5}$$

where $H(z)$ and $\ell(z)$ are as before and

$$s(x, y, t) = \omega\tfrac{2}{3}\Delta_2 h. \tag{4.6}$$

If we substitute the ansatz (4.3), (4.5) into (4.2) and (2.3) and test the result for the former equation with

$$\langle \delta(\tilde{x} - x, \tilde{y} - y)\,\mu(z), 0, 0\rangle \quad \text{and} \quad \langle 0, \delta(\tilde{x} - x, \tilde{y} - y)\,\mu(z), 0\rangle \tag{4.7}$$

and the result for (2.3) with

$$\delta(\tilde{x}-x,\,\tilde{y}-y)\,H(z) \tag{4.8}$$

respectively, we obtain the problem

$$\partial_y^4 U - 24\,\partial_y^2 U + 504\,U + \partial_x^2\left(\partial_y^2 U - 12\,U\right) = -R\,\partial_y\left(60\,h - \frac{3}{2}s\right) + \partial_x\partial_y\left(\Delta_2 V - 12\,V\right), \tag{4.9}$$

$$\partial_x^4 V - 24\,\partial_x^2 V + 504\,V + \partial_y^2\left(\partial_x^2 V - 12\,V\right) = R\,\partial_x\left(60\,h - \frac{3}{2}s\right) + \partial_x\partial_y\left(\Delta_2 U - 12\,U\right), \tag{4.10}$$

$$\partial_t h - \Delta_2 h + \frac{5}{2}h + \frac{9}{448}\left[\left(U\,\partial_y h - V\,\partial_x h\right) + \frac{1}{2}\left(\partial_y U - \partial_x V\right)\,h\right] = \frac{15}{8}s + \frac{5}{448}\left(\partial_y U - \partial_x V\right) \tag{4.11}$$

$$+ \frac{1}{448\cdot 24}\left[\left(U\partial_y s - V\partial_x s\right) - \frac{3}{2}\left(\partial_y U - \partial_x V\right)\,s\right]. \tag{4.12}$$

We solve this system numerically using a finite difference method together with an implicit Euler scheme for the time discretization and a Newton scheme combined with an iterative solver BiCSTAB [37]) for the linear subproblems. We solve the problem with homogeneous Dirichlet boundary conditions on an (L_x, L_y) square. For the initial condition we use

$$h(x,y,0) = xy\left(\frac{x}{L_x} - 1\right)\left(\frac{y}{L_y} - 1\right)10^{-n}, \tag{4.13}$$

where we let $n = 4$. The other variables we set to zero. For all runs we let the Rayleigh number $R = 1.1 * R_c$. For the uncontrolled problem we expect a pattern of square convection cells, for Dirichlet and Neumann boundary conditions on $z = 1/2$ and $z = -1/2$, respectively. Figure 3 shows the streamlines of the vertical velocity. We see in the first column, that after going through a transient phase of a lozenges pattern, square cells start to appear and fill the whole horizontal domain, as expected.

We now ask whether feedback control not only suppresses (or enhances) the instability as well as changes its wavelength, but whether it can also have an effect on the three-dimensional pattern. Starting with the same initial condition, we observe in the right column of figure 3 that for feedback control of $\omega = -0.9$ also here a lozenges pattern appears at first, followed by a pattern of square cells, all having smaller wavelength. Interestingly, at some point, when the amplitude has become large enough, the control effects a change in the up–down symmetry and a new hexagonal pattern eventually establishes itself and remains in this new state. This is a remarkable and new effect and it hints at a nontrivial response of the system with respect to feedback control, that needs to be explored further.

One focus of this study is to rigorously establish the convergence of our Galerkin method before we go into more detail of the bifurcation structure of the reduced model.

5. Convergence

As we have already noted earlier in the text, feedback control may introduce new aspects that need to be dealt with for the expansion of the basis functions. In particular, positive feedback

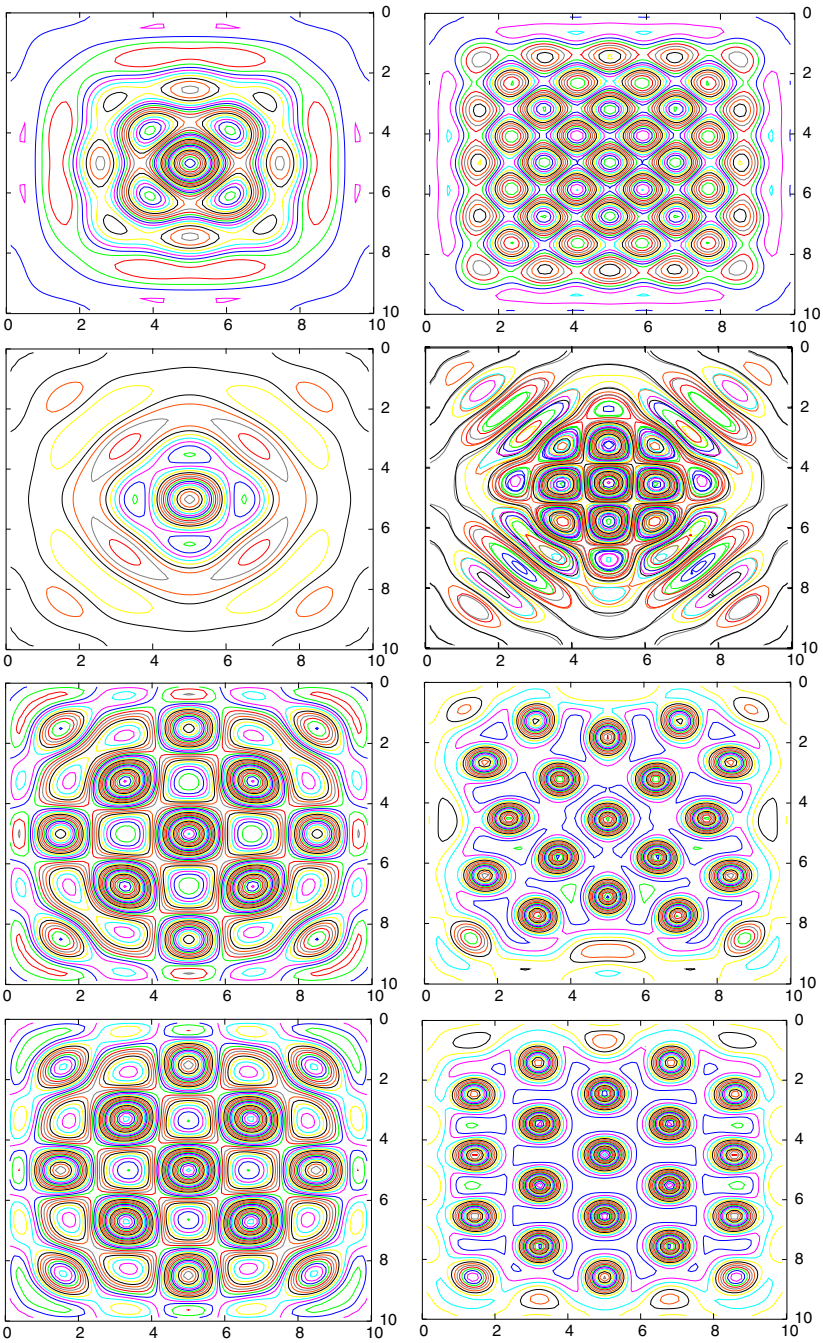

Figure 3. Uncontrolled (left) and controlled ($\omega = -0.9$ right) Rayleigh–Bénard convection for $R = 1.1R_c$

control introduces artificial singularities into the dimension-reduced problem. We note that is already a property of the core problem of the feedback controlled heat equation. We address this problem in the following section and show that additional conditions have to be satisfied, which in turn result in a modification of the basis functions. For the resulting Galerkin scheme we then prove convergence.

5.1. Artificial singularities

We now discuss the problem of artificial singularities for the two-dimensional heat equation with boundary conditions resulting from feedback control. This problem can be further simplified if we Fourier transform it with respect to x,

$$T_t = T_{zz} - k^2\, T, \tag{5.1}$$

$$T_z(1/2, t) = 0, \tag{5.2}$$

$$T_z(-1/2, t) = \omega\, k^2 \int_{-1/2}^{1/2} T \,\mathrm{d}z, \tag{5.3}$$

$$T(z, 0) = g(z). \tag{5.4}$$

Let us assume that this problem has a solution. We can always find a function $\ell(z)$ such that $\ell'(1/2) = 0$ and $\ell'(-1/2) = 0$. Next we can define the following functions

$$s(t) = \omega\, k^2 \int_{-1/2}^{1/2} T \,\mathrm{d}z, \tag{5.5}$$

$$v(z, t) = T(z, t) - \ell(z)\, s(t), \tag{5.6}$$

so that $v(z, t)$ satisfies the equation

$$v_t + \ell\, s_t = v_{zz} - k^2\, v + (\ell'' - k^2\, \ell)\, s \tag{5.7}$$

with homogeneous boundary conditions

$$v_z(1/2, t) = 0, \tag{5.8}$$

$$v_z(-1/2, t) = 0. \tag{5.9}$$

For the initial conditions for v we note that from (5.5)–(5.6)

$$T(z, 0) = g(z) = v(z, 0) + \ell(z)\, s(0), \tag{5.10}$$

$$= v(z, 0) + \ell(z) \frac{\omega k^2}{1 - \rho\omega k^2} \int_{-1/2}^{1/2} v(z, 0) \,\mathrm{d}z, \tag{5.11}$$

where

$$\rho = \int_{-1/2}^{1/2} \ell(z) \,\mathrm{d}z.$$

Integration of (5.11) yields

$$\int_{-1/2}^{1/2} v(z, 0) \,\mathrm{d}z = (1 - \rho\omega\, k^2) \int_{-1/2}^{1/2} g(z) \,\mathrm{d}z$$

and hence

$$v(z, 0) = g(z) - \omega\, k^2 \ell(z) \int_{-1/2}^{1/2} g(z) \,\mathrm{d}z. \tag{5.12}$$

Conversely, it is clear that for given v that satisfies (5.7)–(5.9), with s and ℓ having the above properties, we can define T that satisfies (5.1)–(5.4).

Clearly, if we integrate (5.7) and denote

$$V(t) = \int_{-1/2}^{1/2} v(z,t)\,\mathrm{d}z \qquad \text{and} \qquad \gamma = \int_{-1/2}^{1/2} g(z)\,\mathrm{d}z \tag{5.13}$$

we see immediately that the resulting initial value problem

$$V_t = -(\omega+1)\,k^2\,V \qquad \text{with } V(0) = \gamma(1-\rho\omega k^2) \tag{5.14}$$

will be ill-posed for $\omega < -1$, so this is a property of the full problem and has been explained earlier in [31].

For our Galerkin approximation we proceed in a similar fashion. We approximate $v(z,t)$ by

$$v_N(z,t) = \sum_i^N H_i(z)\,h_i(t), \tag{5.15}$$

where the H_i form a sequence of orthonormal polynomials with respect to the standard inner product,

$$\langle H_i, H_j\rangle = \int_{-1/2}^{1/2} H_i(z)H_j(z)\,\mathrm{d}z = \delta_{ij}, \tag{5.16}$$

which satisfy

$$H_i'(1/2) = 0, \qquad H_i'(-1/2) = 0, \tag{5.17}$$

and set

$$T_N(z,t) = v_N(z,t) + \ell_N(z)\,s(t), \tag{5.18}$$

where $\ell_N(z)$ is a polynomial with

$$\ell_N'(1/2) = 0, \qquad \ell_N'(-1/2) = 1. \tag{5.19}$$

Substitution of (5.18) into (5.1)–(5.3) and taking the inner product with H_j yields for each j the equation

$$h_{j_t} + \langle \ell_N, H_j\rangle\, s_t = \sum_i^N \langle H_i'', H_j\rangle h_i - k^2 h_j + \langle \ell_N'' - k^2\ell_N, H_j\rangle s, \tag{5.20}$$

$$s(t) = \frac{\omega k^2}{1-\rho_N\omega k^2}\int_{-1/2}^{1/2} v_N\,\mathrm{d}z \qquad \text{with } \rho_N = \int_{-1/2}^{1/2} \ell_N\,\mathrm{d}z. \tag{5.21}$$

The problem for $v_N(z,t)$ is now obtained by summation of the product of H_j and (5.20). If we integrate the resulting equation by using (5.21) as well as the properties of H_i and ℓ_N and denote

$$V_N(t) = \int_{-1/2}^{1/2}\sum_j^N H_j\,h_j\,\mathrm{d}z = \int_{-1/2}^{1/2} v_N\,\mathrm{d}z, \tag{5.22}$$

and the projection

$$P(Q) = \sum_i^N \langle Q, H_j\rangle H_j, \tag{5.23}$$

for some polynomial Q, we obtain the following equation

$$\left[1+\omega k^2\left(\int_{-1/2}^{1/2} P(\ell_N)-\rho_N\,\mathrm{d}z\right)\right] V_{Nt} = -k^2\left[1+\omega+\omega k^2\left(\int_{-1/2}^{1/2} P(\ell_N)-\rho_N\,\mathrm{d}z\right)\right] V_N$$
$$+\omega k^2\left[\int_{-1/2}^{1/2} P(\ell_N^{''})-\ell_N^{''}\,\mathrm{d}z\right] V_N+\left(1-\rho_N\omega k^2\right)\int_{-1/2}^{1/2}\sum_i^N\left[P(H_i^{''})-H_i^{''}\right]h_i\,\mathrm{d}z.$$

In this form, we observe that, for $\omega < 0$, the approximate problem will produce artificial singularities, which are not present in the exact problem, if

$$1+\omega k^2\left(\int_{-1/2}^{1/2} P(\ell_N)-\rho_N\,\mathrm{d}z\right)=0.$$

However, the sequence of orthonormal polynomials H_i that produce the approximation v_N, all have property (5.17). Hence the constant polynomial $H_0(z)=1$ is always a member. But this means that

$$\int_{-1/2}^{1/2} P(Q)\,\mathrm{d}z=\langle Q,H_0\rangle=\int_{-1/2}^{1/2} Q\,\mathrm{d}z. \tag{5.24}$$

Therefore, (5.24) reduces to

$$V_{Nt}=-(1+\omega)\,k^2\,V_N \qquad \text{with } V_N(0)=\gamma(1-\rho_N\omega k^2). \tag{5.25}$$

Property (5.24), however, is not necessarily satisfied for general boundary condition. If we change, for example, the top ($z=1/2$) boundary condition to be of the Dirichlet type, then $H_i(1/2)=0$ and (5.24) cannot be derived anymore. Therefore, if we want to approximate problem (5.1)–(5.4) with $T(1/2,t)=0$, by (5.15)–(5.19) with $H_i(1/2)=0$ and $\ell_N(1/2)=0$, we again find the same coefficient of V_{Nt}. In this case, however, we have to explicitly require

$$\int_{-1/2}^{1/2}\ell_N\,\mathrm{d}z=\int_{-1/2}^{1/2} P(\ell_N)\,\mathrm{d}z \tag{5.26}$$

in order to avoid artificial singularities for negative ω. This in turn gives an additional constraint on ℓ_N, leading to the new basis function (2.21).

5.2. *Convergence proof*

For the problem

$$T_t=T_{xx}+T_{zz} \qquad \text{on } \Omega, \tag{5.27}$$

$$T_z(x,1/2,t)=0, \tag{5.28}$$

$$T_z(x,-1/2,t)=-\omega\int_{-1/2}^{1/2} T_{xx}\,\mathrm{d}z, \tag{5.29}$$

$$T(x,z,0)=g(x,z), \tag{5.30}$$

where Ω denotes the domain $]0,L[\times]-1/2,1/2[$, and where T satisfies periodic boundary conditions in x, and $t\in[0,t_f]$, we analyse the convergence properties of a Galerkin scheme designed to approximate the solution of (5.27)–(5.30). For later use, we set $I:=]-1/2,1/2[$. For this purpose, we first make some assumptions regarding the solution of the continuous problem. We will assume that for $\omega>-1$ the problem has, for sufficiently smooth data g, a unique solution with $T\in L^2(H^2(\Omega))$, and that this solution has additional regularity properties, T and $T_t\in L^2(H^{7/2}(\Omega))$.

In the next paragraph, we reformulate the continuous problem by splitting T into two variables, θ, that satisfies homogeneous boundary conditions at $z = \pm 1/2$, and a second term $s(x,t)l(z)$ which accounts for the control boundary conditions (5.29). We also pass to the Fourier-transform with respect to x. In section 5.2.2, we will set up the weak formulation and the Galerkin scheme. In section 5.2.3 we derive estimates for the difference of the solution T and the discrete solution T^N in terms of the norm of the continuous solution for θ. The bound for the difference of T and T^N provided by this estimate tends to zero as N tends to ∞, where N is the dimension of the sub-space used for the discretization.

5.2.1. Reformulation. Now fix a polynomial $l(z)$ so that

$$l'(1/2) = 0, \qquad l'(-1/2) = 1 \qquad \text{and} \qquad \int_{-1/2}^{1/2} l \, \mathrm{d}z = 0,$$

and let

$$s(x,t) = T_z(x,-1/2,t), \tag{5.31}$$

$$\theta(x,z,t) = T(x,z,t) - s(x,t)l(z) \tag{5.32}$$

for $t \geqslant 0$. Then, s and θ, θ_t are in $L^2(H^2(]0,L[))$ and $L^2(H^2(\Omega))$, respectively, and satisfy

$$\theta_t + s_t l = \theta_{xx} + \theta_{zz} + s_{xx} l + s l'', \tag{5.33}$$

$$s = -\omega \int_{-1/2}^{1/2} \theta_{xx} \, \mathrm{d}z, \tag{5.34}$$

$$\theta_z(x, \pm 1/2, t) = 0, \tag{5.35}$$

$$s(x,0) = g_z(x,-1/2), \tag{5.36}$$

$$\theta(x,z,0) = g(x,z) - s(x,0)l(z). \tag{5.37}$$

Conversely, any solution s and θ of (5.33)–(5.37) of this regularity class generates via

$$T(x,z,t) = \theta(x,z,t) + s(x,t)l(z) \tag{5.38}$$

a solution of (5.27)–(5.30) within the class $L^2(H^2(\Omega))$ (or better). Since we assumed that the solution T of (5.27)–(5.30) is unique, the solution s and θ of (5.33)–(5.37) must be unique too. For, assume we have two solutions, s_1, θ_1 and s_2, θ_2, then from uniqueness of T, it follows

$$\theta_1(x,z,t) + s_1(x,t)l(z) = \theta_2(x,z,t) + s_2(x,t)l(z). \tag{5.39}$$

Evaluating this at $z = -1/2$ yields $s_1 = s_2$ and plugging this into (5.39) yields $\theta_1 = \theta_2$.

In the following, we will assume that the solution (5.33)–(5.37) has additional regularity properties,

$$s(t) \in H^2(]0,L[) \qquad \text{and} \qquad \theta(t) \in H^2(\Omega) \qquad \text{both for all } t \in [0, t_f]. \tag{5.40}$$

We now Fourier transform (5.33)–(5.37), via

$$s(x,t) = \sum_{j=0}^{\infty} \hat{s}(j,t) \mathrm{e}^{\mathrm{i}k_j x}, \qquad \theta(x,z,t) = \sum_{j=0}^{\infty} \hat{\theta}(j,z,t) \mathrm{e}^{\mathrm{i}k_j x} \qquad \text{with } k_j = \frac{2\pi}{L} j.$$

In the following, we will typically suppress the dependence on j, e.g. by writing k instead of k_j. The transformed equations then read

$$\hat{\theta}_t + \hat{s}_t l = -k^2\hat{\theta} + \hat{\theta}_{zz} - k^2\hat{s}l + \hat{s}l'', \qquad \text{on } I, \text{ and for } t > 0 \tag{5.41}$$

$$\hat{s} = \omega k^2 \int_{-1/2}^{1/2} \hat{\theta}\, \mathrm{d}z, \qquad \text{on } I, \text{ and for } t > 0, \tag{5.42}$$

$$\hat{\theta}_z(j, \pm 1/2) = 0, \tag{5.43}$$

$$\hat{s}(j, 0) = \hat{g}_z(j, -1/2), \tag{5.44}$$

$$\hat{\theta}(j, z, 0) = \hat{g}(j, z) - \hat{s}(j, 0)l(z). \tag{5.45}$$

These equations have to be solved for all $j = 0, 1, \ldots$. From our above considerations, we conclude that (5.41)–(5.45) can be assumed to have, for each j, a unique solution $\hat{s}, \hat{\theta}$ within the class of functions that satisfy

$$\hat{\theta}(t) \in H^2(I), \qquad \text{for all } t \in [0, t_f] \tag{5.46}$$

and

$$\int_0^{t_f} |\hat{s}|^2 \,\mathrm{d}t < \infty \qquad \text{and} \qquad \hat{\theta} \in L^2H^2(I)).$$

5.2.2. Weak formulation and discretization. Let

$$\mathcal{M}_c := \{\psi \in H^2(I);\ \psi_z(\pm 1/2) = 0\}.$$

Then, for the above solution we have $\hat{\theta}(t) \in \mathcal{M}_c$ and $\hat{\theta}, \hat{s}$ satisfy (where $(\cdot, \cdot)$ denotes the inner product of $L^2(I)$),

$$(\hat{\theta}_t, \psi) + \hat{s}_t(l, \psi) = -(\hat{\theta}_z, \psi_z) - \hat{s}(l', \psi_z) - \hat{s}\psi(-1/2) - k^2(\hat{\theta}, \psi) - k^2\hat{s}(l, \psi),$$

$$\text{for all } \psi \in \mathcal{M}_c. \tag{5.47}$$

The remaining conditions, (5.42)–(5.45), carry over from before.

For the discrete subspaces of $\mathcal{M}_c$, we take

$$\mathcal{M}_N := \mathrm{span}\{\mathcal{H}_0, \mathcal{H}_1, \ldots, \mathcal{H}_N\},$$

where $\mathcal{H}_i$ are polynomials in z, ordered by their degree, that satisfy

$$\mathcal{H}_i'(\pm 1/2) = 0, \qquad (\mathcal{H}_i, \mathcal{H}_j) = \delta_{ij}. \tag{5.48}$$

Note that, in particular, $\mathcal{H}_0 \equiv 1$. We then formulate the following problem (discretized with respect to z):

Find $\hat{s}^N, \hat{\theta}^N$, with $\hat{\theta}^N(t) \in \mathcal{M}_N$, so that

$$(\hat{\theta}_t^N, \psi) + \hat{s}_t^N(l, \psi) = -(\hat{\theta}_z^N, \psi_z) - \hat{s}^N(l', \psi_z) - \hat{s}^N\psi(-1/2) - k^2(\hat{\theta}^N, \psi) - k^2\hat{s}^N(l, \psi),$$

$$\text{for all } \psi \in \mathcal{M}_N, \tag{5.49}$$

$$\hat{s}^N = \omega k^2 \int_{-1/2}^{1/2} \hat{\theta}^N \,\mathrm{d}z \tag{5.50}$$

$$\hat{s}^N(j, 0) = \hat{s}(j, 0) \tag{5.51}$$

$$\hat{\theta}^N(j, z, 0) = \sum_{i=0}^{N} (\hat{\theta}(j, \cdot, 0), \mathcal{H}_i)\, \mathcal{H}_{i(z)}. \tag{5.52}$$

By setting $\psi = 1$ in (5.47) and in (5.49), respectively, we find that $\hat{s}$ and $\hat{s}^N$ satisfy the same equation,

$$\hat{s}_t = -(1+\omega)k^2\hat{s} \qquad \text{and} \qquad \hat{s}^N_t = -(1+\omega)k^2\hat{s}^N,$$

so that in view of (5.51), we get $\hat{s}(j,t) = \hat{s}^N(j,t)$ for all $t \in [0, t_f]$. Therefore, when we subtract (5.47) and (5.49), all $\hat{s}$ and $\hat{s}^N$ terms cancel

$$(\hat{\theta}_t - \hat{\theta}^N_t, \psi) = -(\hat{\theta}_z - \hat{\theta}^N_z, \psi_z) - k^2(\hat{\theta} - \hat{\theta}^N, \psi). \tag{5.53}$$

5.2.3. Error analysis. Let $\pi_N : \mathcal{M}_c \to \mathcal{M}_N$ denote a projection onto $\mathcal{M}_N$, and let

$$\hat{\zeta} := \hat{\theta} - \pi_N(\hat{\theta}), \qquad \hat{\zeta}^N := \hat{\theta}^N - \pi_N(\hat{\theta}).$$

Using this, (5.53) becomes

$$(\hat{\zeta}_t - \hat{\zeta}^N_t, \psi) = -(\hat{\zeta}_z - \hat{\zeta}^N_z, \psi_z) - k^2(\hat{\zeta} - \hat{\zeta}^N, \psi).$$

For the special choice $\psi = \hat{\zeta}^N$, this becomes

$$(\hat{\zeta}_t, \hat{\zeta}^N) - \frac{1}{2}\frac{\mathrm{d}}{\mathrm{d}t}||\hat{\zeta}^N||^2 = -(\hat{\zeta}_z, \hat{\zeta}^N_z) + ||\hat{\zeta}^N_z||^2 - k^2(\hat{\zeta}, \hat{\zeta}^N) + k^2||\hat{\zeta}^N||^2.$$

By an application of the Cauchy–Schwarz inequality, and Young's inequality, we get

$$\frac{\mathrm{d}}{\mathrm{d}t}||\hat{\zeta}^N||^2 + ||\hat{\zeta}^N_z||^2 + k^2||\hat{\zeta}^N||^2 \leqslant ||\hat{\zeta}_t||^2 + ||\hat{\zeta}_z||^2 + k^2||\hat{\zeta}||^2 + ||\hat{\zeta}^N||^2. \tag{5.54}$$

Here as further below, the unspecified norm denotes the $L^2(I)$-norm.

If we forget for the moment the second and third terms on the left-hand side in (5.54), we can use Gronwall's lemma to get an estimate for $||\hat{\zeta}_N||^2$,

$$||\hat{\zeta}^N||^2 \leqslant ||\hat{\zeta}^N(0)||^2\mathrm{e}^t + \int_0^t (||\hat{\zeta}_t||^2 + ||\hat{\zeta}_z||^2 + k^2||\hat{\zeta}||^2)\mathrm{e}^{t-s}\,\mathrm{d}s$$

$$\leqslant (t+1)\mathrm{e}^t\left[||\hat{\zeta}^N(0)||^2 + \int_0^t \left(||\hat{\zeta}_t||^2 + ||\hat{\zeta}_z||^2 + k^2||\hat{\zeta}||^2\right)\mathrm{d}t\right].$$

Recall now that for $t = 0$, $\hat{\theta}^N$ was chosen to be the $L^2(I)$ projection of $\hat{\theta}$, see (5.52). From this, we conclude

$$\begin{aligned}||\hat{\zeta}^N(0)||^2 &= ||\hat{\theta}^N(0) - \pi_N(\hat{\theta}(0))||^2 \\ &= \left(\hat{\theta}^N(0) - \pi_N(\hat{\theta}(0)), 2\hat{\theta}(0) - 2\hat{\theta}^N(0) + \hat{\theta}^N(0) - \pi_N(\hat{\theta}(0))\right).\end{aligned}$$

Note that the inserted terms do not contribute to the right-hand side, because of the choice of $\hat{\theta}^N$ as $L^2(I)$-projection of $\hat{\theta}(0)$ onto $\mathcal{M}_N$, i.e. $(\hat{\theta}^N(0) - \pi_N(\hat{\theta}(0)),\ 2\hat{\theta}(0) - 2\hat{\theta}^N(0)) = 0$. Hence, we have that the last equation is

$$\begin{aligned}&= \left(\hat{\theta}^N(0) - \pi_N(\hat{\theta}(0)), 2\hat{\theta}(0) - \pi_N(\hat{\theta}(0)) - \hat{\theta}^N(0)\right), \\ &= ||\hat{\theta}(0) - \pi_N(\hat{\theta}(0)||^2 - ||\hat{\theta}(0) - \hat{\theta}^N(0)||^2, \\ &\leqslant ||\hat{\theta}(0) - \pi_N(\hat{\theta}(0)||^2 = ||\hat{\zeta}(0)||^2,\end{aligned}$$

so that

$$||\hat{\zeta}^N||^2 \leqslant (t+1)\mathrm{e}^t\left[||\hat{\zeta}(0)||^2 + \int_0^t \left(||\hat{\zeta}_t||^2 + ||\hat{\zeta}_z||^2 + k^2||\hat{\zeta}||^2\right)\mathrm{d}t\right]. \tag{5.55}$$

Evaluating the right-hand side at $t = t_f$ and plugging the result into (5.54), we get

$$\frac{\mathrm{d}}{\mathrm{d}t}||\hat{\xi}^N||^2 + ||\hat{\xi}^N_z||^2 + k^2||\hat{\xi}^N||^2 \leqslant ||\hat{\xi}_t||^2 + ||\hat{\xi}_z||^2 + k^2||\hat{\xi}||^2 + (t_f + 1)\mathrm{e}^{t_f}\left[||\hat{\xi}(0)||^2 + \int_0^{t_f}\left(||\hat{\xi}_t||^2 + ||\hat{\xi}_z||^2 + k^2||\hat{\xi}||^2\right)\mathrm{d}t\right].$$

Integrating over $[0, t]$, we get after a little algebra

$$\sup_{0\leqslant t\leqslant t_f}||\hat{\xi}^N||^2 + \int_0^{t_f}\left(||\hat{\xi}^N_z||^2 + k^2||\hat{\xi}^N||^2\right)\mathrm{d}t \leqslant 2(1 + t_f^2\mathrm{e}^{t_f})\left[||\hat{\xi}(0)||^2 + \int_0^{t_f}\left(||\hat{\xi}_t||^2 + ||\hat{\xi}_z||^2 + k^2||\hat{\xi}||^2\right)\mathrm{d}t\right].$$

In short,

$$||\hat{\xi}^N||^2_{L^\infty(L^2(I))} + ||\hat{\xi}^N_z||_{L^2(L^2(I))} + k^2||\hat{\xi}^N||_{L^2(L^2(I))} \leqslant C(t_f)\left(||\hat{\xi}(0)||^2 + ||\hat{\xi}_t||^2_{L^2(L^2(I))} + ||\hat{\xi}_z||^2_{L^2(L^2(I))} + k^2||\hat{\xi}||^2_{L^2(L^2(I))}\right).$$

We are now in a position to estimate $T - T^N$, where T^N can be reconstructed from the discrete solutions θ^N and s^N via

$$T^N(x,\ t) = \theta^N(x, z, t) + s^N(x, t)l(z),$$

$$\theta^N(x, z, t) = \sum_{j=0}^{\infty}\hat{\theta}^N(j, z, t)\mathrm{e}^{\mathrm{i}k_j x},$$

$$s^N(x, t) = \sum_{j=0}^{\infty}\hat{s}^N(j, t)\mathrm{e}^{\mathrm{i}k_j x}.$$

Using our finding that $\hat{s} = \hat{s}^N$, we conclude

$$\begin{aligned}
&||T - T^N||^2_{L^\infty(L^2(\Omega))} + ||T - T^N||^2_{L^2(H_1(\Omega))}\\
&\quad = ||\theta - \theta^N||^2_{L^\infty(L^2(\Omega))} + ||\theta - \theta^N||^2_{L^2(H_1(\Omega))}\\
&\quad \leqslant ||\zeta||^2_{L^\infty(L^2(\Omega))} + ||\zeta^N||^2_{L^\infty(L^2(\Omega))} + ||\zeta||^2_{L^2(H_1(\Omega))} + ||\zeta^N||^2_{L^2(H_1(\Omega))}\\
&\quad \leqslant \sum_{j=0}^{\infty}\Big[||\hat{\xi}||^2_{L^\infty(L^2(I))} + ||\hat{\xi}^N||^2_{L^\infty(L^2(I))} + ||\hat{\xi}||^2_{H^1(L^2(I))} + ||\hat{\xi}^N_z||^2_{L^2(L^2(I))}\\
&\qquad + (1 + k^2)||\hat{\xi}^N||^2_{L^2(L^2(I))}\Big].
\end{aligned}$$

The terms on the right-hand side containing $\hat{\xi}^N$ can be estimated using (5.55) and (5.56); this introduces $||\hat{\xi}(0)||^2$. We wish to replace this term (and $||\hat{\xi}||^2_{L^\infty(L^2(I))}$) by L^2-estimates of $\hat{\xi}_t$, in the following manner: let $\tilde{t} \in [0, t_f]$ be chosen so that

$$\left|\left|\hat{\xi}(\tilde{t})\right|\right|^2_{L^2(I)} = \min_{t\in[0,t_f]}\left|\left|\hat{\xi}(t)\right|\right|^2_{L^2(I)} \leqslant \frac{1}{t_f}\int_0^{t_f}\left|\left|\hat{\xi}(t)\right|\right|^2_{L^2(I)}.$$

Then, we get

$$\begin{aligned}
\left|\left|\hat{\xi}(t)\right|\right|^2_{L^2(I)} &= \left|\left|\hat{\xi}(\tilde{t})\right|\right|^2_{L^2(I)} + \int_{\tilde{t}}^{t} 2(\hat{\xi}_t(s), \hat{\xi}(s))\,\mathrm{d}s\\
&\leqslant \frac{1}{t_f}\int_0^{t_f}\left|\left|\hat{\xi}(t)\right|\right|^2_{L^2(I)} + \int_t^{t_f}\left(\left|\left|\hat{\xi}_t(s)\right|\right|^2_{L^2(I)} + \left|\left|\hat{\xi}(s)\right|\right|^2_{L^2(I)}\right)\mathrm{d}s\\
&\leqslant (1 + 1/t_f)\int_t^{t_f}\left(\left|\left|\hat{\xi}_t(s)\right|\right|^2_{L^2(I)} + \left|\left|\hat{\xi}(s)\right|\right|^2_{L^2(I)}\right)\mathrm{d}s.
\end{aligned}$$

Setting $t = 0$ on the left-hand side yields the estimate for $||\hat{\zeta}(0)||^2$. Furthermore, taking the supremum on the right-hand side, we get

$$||\hat{\zeta}||^2_{L^\infty(L^2(I))} \leqslant (1 + 1/t_f)\left(||\hat{\zeta}_t||_{L^2(L^2(I))} + ||\hat{\zeta}||_{L^2(L^2(I))}\right). \tag{5.56}$$

Now, using (5.55) and (5.56), we get

$$||T - T^N||^2_{L^\infty(L^2(\Omega))} + ||T - T^N||^2_{L^2(H_1(\Omega))}$$
$$\leqslant C(t_f)\sum_{j=0}^{\infty}\left(||\hat{\zeta}_t||^2_{L^2(L^2(I))} + ||\hat{\zeta}_z||^2_{L^2(L^2(I))} + k^2||\hat{\zeta}||^2_{L^2(L^2(I))}\right). \tag{5.57}$$

We will now make a special choice for π_N. Let, for $N > 0$,

$$\text{proj}_N : \{\psi_z;\ \psi \in \mathcal{M}_c\} \to \{\psi_z;\ \psi \in \mathcal{M}_N\}$$

be the interpolation operator which assigns, to every function h from the left set, the polynomial which interpolates this function at the $N + 1$ Gauss–Lobatto nodes. Note that this polynomial has degree $N+1$, and since the left and right end points of I are included in the Gauss–Lobatto nodes, it is zero at $\pm 1/2$. In other words, it arises as the derivative of a polynomial of degree $N + 2$ with vanishing derivatives at $z = \pm 1/2$, i.e. as the derivative of a polynomial of $\mathcal{M}_N$. So, proj_N is well defined. We know from [38] that

$$\left|\left|h - \text{proj}_N(h)\right|\right|_{L^2(I)} \leqslant CN^{-1}||h||_{H^1(I)}. \tag{5.58}$$

We now define π_N to be, for $f \in \mathcal{M}_c$,

$$\pi_0(f) = f(-1/2),$$
$$\pi_N(f) = f(-1/2) + \int_{-1/2}^{z} \text{proj}_N(f_z)\,\mathrm{d}z, \qquad \text{for } N > 0.$$

From the construction of proj_N it is easy to see that $\pi_N(f) \in \mathcal{M}_N$. Since

$$f - \pi_N(f) = \int_{-1/2}^{z} f_z - \text{proj}_N(f_z)\,\mathrm{d}z$$

we get from (5.58)

$$||(f - \pi_N(f))_z||_{L^2(I)} = \left|\left|f_z - \text{proj}_N(f_z)\right|\right|_{L^2(I)} \leqslant CN^{-1}||f_z||_{H^1(I)}$$

and, with a little algebra using Cauchy–Schwarz

$$\begin{aligned}||f - \pi_N(f)||_{L^2(I)} &\leqslant \left|\left|f_z - \text{proj}_N(f_z)\right|\right|_{L^2(I)}\\ &\leqslant CN^{-1}||f_z||_{H^1(I)}\\ &\leqslant CN^{-1}||f||_{H^2(I)}.\end{aligned}$$

Furthermore, if in addition to $f(t) \in \mathcal{M}_c$ we also have $f_t(t) \in H^2(I)$, we obtain the estimate

$$||(f - \pi_N(f))_t||_{L^2(I)} = ||f_t - \pi_N(f_t)||_{L^2(I)} \leqslant CN^{-1}||f_t||_{H^2(I)}.$$

We use this to get

$$||T - T^N||^2_{L^\infty(L^2(\Omega))} + ||T - T^N||^2_{L^2(H_1(\Omega))}$$
$$\leqslant C(t_f)\,N^{-1}\sum_{j=0}^{\infty}\left(||\hat{\theta}_t||^2_{L^2(H^2(I))} + ||\hat{\theta}_z||^2_{L^2(H^1(I))} + k^2||\hat{\theta}||^2_{L^2(H^2(I))}\right)$$
$$\leqslant C(t_f)\,N^{-1}\left(||\theta_t||^2_{L^2(H^2(\Omega))} + ||\theta||^2_{L^2(H^2(\Omega))}\right). \tag{5.59}$$

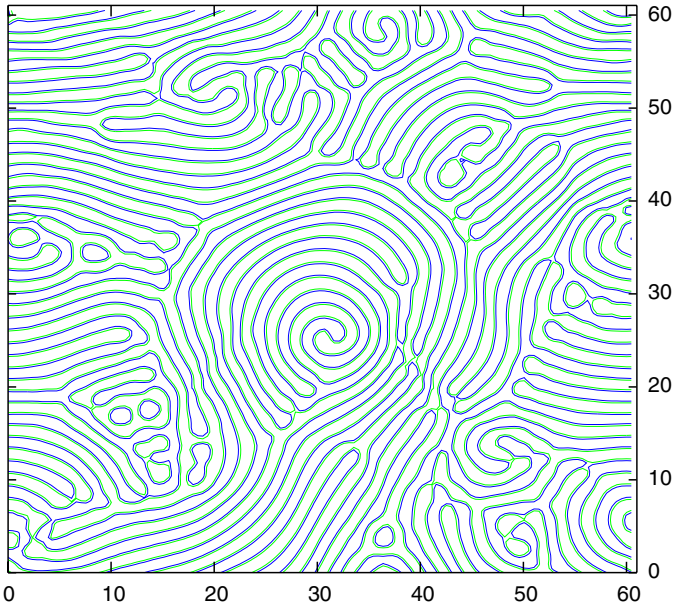

Figure 4. Streamlines of the temperature at $z = -1/5$ and $z = 1/2$ for $Pr = 1$ and $R = 1.7 \cdot 1776 = 1.7 \cdot R_c$.

6. Outlook and discussion

In this study we discussed some basic aspects of feedback controlled Rayleigh–Bénard convection via an appropriate Galerkin approximation. This approximation arose as a result of the analysis of the problem of artificial singularities for positive feedback control.

It would be interesting to develop this method further. A natural next step is feedback control of large-aspect ratio dynamics such as the well-known spiral-defect chaos. In fact it is straightforward to derive the dimension-reduced model for spiral-defect chaos.

For this problem we cannot neglect the left-hand side of (2.1). In the flow regime considered here, the Prandtl number is of O(1). Also here, the boundary conditions at $z = \pm 1/2$ are both homogeneous Neumann conditions, so that in our Galerkin approximation the minimal set are two temperature functions to capture the vertical structure of the flow. Otherwise, we proceed similarly as before and make the following ansatz

$$\phi = U(x, y, t)\,\mu(z), \qquad \varphi = V(x, y, t)\,\mu(z), \qquad \psi = W(x, y, t)\,\nu(z) \tag{6.1}$$

$$T = hH_0 + fH_1, \qquad H_0 = \nu, \quad H_1 = \mu_z, \qquad \int_{-1/2}^{1/2} H_0 H_1 \,\mathrm{d}z \tag{6.2}$$

where

$$\nu = \frac{1}{2}\left(z^2 - \frac{1}{4}\right), \qquad \mu = \nu^2, \tag{6.3}$$

and arrive at the Galerkin approximation

$$
\begin{aligned}
&12\partial_t U - \partial_t(\partial_y^2 U - \partial_x\partial_y V) - \frac{5}{44}\partial_y(\partial_y W(\partial_x^2 V - \partial_x\partial_y U) + \partial_x W(\partial_y^2 U - \partial_x\partial_y V)) \\
&\quad - \frac{1}{2}\partial_y(V\partial_y W + U\partial_x W) + \frac{1}{2}\partial_x W(\partial_x V - \partial_y U) - \partial_y W(\partial_x U + \partial_y V) - V\Delta_2 W \\
&\quad = -Pr\left[\partial_y^4 U - 24\,\partial_y^2 U + 504\,U + \partial_x^2\left(\partial_y^2 U - 12\,U\right) + R\,9\,\partial_y h - \partial_x\partial_y\left(\Delta_2 V - 12\,V\right)\right],
\end{aligned}
\tag{6.4}
$$

$$
\begin{aligned}
&12\,\partial_t V - \partial_t(\partial_x^2 V - \partial_x\partial_y U) + \frac{5}{44}\partial_x\left(\partial_y W(\partial_x^2 V - \partial_x\partial_y U) + \partial_x W(\partial_y^2 U - \partial_x\partial_y V)\right) \\
&\quad + \frac{1}{2}\partial_x(V\partial_y W + U\partial_x W) + \frac{1}{2}\partial_y W(\partial_x V - \partial_y U) + \partial_x W(\partial_x U + \partial_y V) + U\Delta_2 W \\
&\quad = -Pr[\partial_x^4 V - 24\,\partial_x^2 V + 504\,V + \partial_y^2\left(\partial_x^2 V - 12\,V\right) - R\,9\,\partial_x h - \partial_x\partial_y\left(\Delta_2 U - 12\,U\right)],
\end{aligned}
\tag{6.5}
$$

$$
\begin{aligned}
&\partial_t\Delta W + \frac{3}{28}\left(\partial_x W\partial_y\Delta W - \partial_y W\partial_x\Delta W\right) + \frac{1}{56}\partial_x\left(U(\partial_y U - \partial_x V)\right) \\
&\quad + \frac{1}{56}\partial_y\left(V(\partial_y U - \partial_x V)\right) - \frac{1}{84}\partial_x\left(V(\partial_x U + \partial_y V)\right) + \frac{1}{84}\partial_y\left(U(\partial_x U - \partial_y V)\right) \\
&\quad = Pr\left(\Delta^2 W - 10\,\Delta W\right),
\end{aligned}
\tag{6.6}
$$

$$
\begin{aligned}
&\partial_t h + \frac{3}{28}\left(\partial_x W\partial_y h - \partial_y W\partial_x h\right) + \frac{1}{84}\left(V\partial_x f - U\partial_y f\right) + \frac{1}{56}(\partial_x V - \partial_y U)f \\
&\quad = \Delta h - 10\,h - \frac{3}{28}(\partial_x V - \partial_y U),
\end{aligned}
\tag{6.7}
$$

$$
\partial_t f + \frac{1}{12}\left(\partial_x W\partial_y f - \partial_y W\partial_x f\right) + \frac{1}{12}\left(V\partial_x h - U\partial_y h\right) - \frac{1}{24}(\partial_x V - \partial_y U)h = \Delta h - 42\,h.
\tag{6.8}
$$

We solve this system using a pseudo-spectral method and the implicit Euler method for the time discretization. We choose periodic boundary conditions for the horizontal boundaries. We set $Pr = 1$ and $R = 1776 \cdot 1.7 = R_c * 1.7$. In figure 4 we see a snapshot of the streamlines for the temperature. It would now be interesting to include feedback control and explore its impact on the evolving pattern. The results for the controlled 3D Rayleigh–Bénard convection have already shown that it is not quite obvious which state the system will enter and needs to be carefully investigated. We note that in view of the results of [17] with respect to the problems of the generalized Swift–Hohenberg model to correctly describe the evolution of spiral-defect chaos, and on the basis of the results on feedback-controlled Rayleigh–Bénard convection of this study, the Galerkin approximation, as discussed here, is a suitable and well-founded method for the numerical investigation of feedback-controlled spiral-defect chaos.

Appendix A. Galerkin approximation with two temperature functions for controlled Rayleigh–Bénard convection

Appendix A.1. Governing equations

Here, we derive the Galerkin approximation with two temperature functions. We let

$$
T(x, z, t) = h(x, t)\,H_0(z) + f(x, t)\,H_1(z) + s(x, t)\,\ell_2(z),
\tag{A.1}
$$

where $H_0(z)$ and $H_1(z)$ are chosen such that $H_0(1/2) = 0$ and $H_0'(-1/2) = 0$ which yields a second order polynomial, while the same conditions for $H_1(z)$ together with

$$\langle H_0, H_1 \rangle = 0 \tag{A.2}$$

yield a third order polynomial. We arrive at

$$H_0(z) = \left(z - \frac{1}{2}\right)\left(z + \frac{3}{2}\right), \tag{A.3}$$

$$H_1(z) = \left(z - \frac{1}{2}\right)\left(z^2 + \frac{29}{32}z + \frac{7}{64}\right). \tag{A.4}$$

The polynomial $\ell_2(z)$ naturally must satisfy $\ell_2(1/2) = 0$. The order will be further increased by requiring the boundary condition at $z = -1/2$ to be satisfied. However, when considering the possibility of negative gain $\omega < 0$ we obtain artificial singularities, not present in the full problem, unless

$$\rho_2 = \int_{-1/2}^{1/2} \ell_2(z)\,\mathrm{d}z = \langle \ell_2, H_0 \rangle \int_{-1/2}^{1/2} H_0(z)\,\mathrm{d}z + \langle \ell_2, H_1 \rangle \int_{-1/2}^{1/2} H_1(z)\,\mathrm{d}z$$

is satisfied. Calculations can be further simplified, if we choose $\ell_2(z)$ to also be orthogonal to H_0 and H_1. As a consequence, we obtain a polynomial of fourth order such that $\rho_2 = 0$ and normalize it such that $\ell_2'(-1/2) = 1$. This yields

$$\ell_2(z) = -\frac{7}{4}\left(z - \frac{1}{2}\right)\left(z^3 + \frac{1}{10}z^2 - \frac{17}{140}z - \frac{1}{280}\right). \tag{A.5}$$

For the velocity function we require $\boldsymbol{u}$ to be divergence free. Additionally, we require no-slip boundary conditions at $z = 1/2$ and $z = -1/2$. This yields

$$v(x, z, t) = u(x, t)\,\mu_z(z), \qquad w(x, z, t) = -u_x(x, t)\,\mu(z), \tag{A.6}$$

where

$$\mu(z) = \frac{1}{4}\left(z^2 - \frac{1}{4}\right)^2. \tag{A.7}$$

We can now derive the Galerkin approximation by testing the full problem with the test functions

$$\theta_0 = \delta(x)\,\mu_z(z), \qquad \theta_1 = -\delta'(x)\,\mu_z(z), \tag{A.8}$$

$$\phi_0 = \delta(x) H_0(z), \qquad \phi_1 = \delta(x) H_1(z), \tag{A.9}$$

to obtain

$$u_{xxxx} - 24\,u_{xx} + 504\,u = -R\left(60\,h + \frac{27}{8}\,f - \frac{1}{5}\,s\right)_x, \tag{A.10}$$

$$h_t - h_{xx} + \frac{5}{2}\,h + \frac{9}{448}\left(h_x u + \frac{1}{2}\,h u_x\right) = -\frac{5}{64}\,f + \frac{15}{8}\,s + \frac{5}{448}\,u_x + \frac{1}{448}\left(\frac{97}{96} f_x u + \frac{91}{64}\,f u_x\right) + \frac{1}{448 \cdot 20}\left(3\,s_x u + \frac{37}{12}\,s u_x\right), \tag{A.11}$$

$$f_t - f_{xx} + \frac{3059}{130}\,f - \frac{173}{390 \cdot 32}\left(f_x u + \frac{1}{2}\,f u_x\right) = -\frac{112}{13}\,h - \frac{6132}{325}\,s + \frac{9}{130}\,u_x + \frac{1}{390}\left(97\,h_x u - \frac{79}{2}\,h u_x\right) + \frac{1}{429 \cdot 200}\left(31\,s_x u + \frac{3 \cdot 329}{4}\,s u_x\right), \tag{A.12}$$

with

$$s = \omega \left(\frac{2}{3} h_{xx} + \frac{1}{48} f_{xx} \right). \tag{A.13}$$

Appendix A.2. Linear stability for two temperature functions

We first like to determine the critical Raleigh number (R_c) of the above problem. We linearize about the conductive state, hence about $u(x,t) = 0$, $h(x,t) = 0$, $f(x,t) = 0$ and $s(x,t) = 0$.

$$u_{xxxx} - 24\, u_{xx} + 504\, u = -R \left(60\, h + \frac{27}{8} f - \frac{1}{5} s \right)_x, \tag{A.14}$$

$$h_t - h_{xx} + \frac{5}{2} h = -\frac{5}{64} f + \frac{15}{8} s + \frac{5}{448} u_x, \tag{A.15}$$

$$f_t - f_{xx} + \frac{3059}{130} f = -\frac{112}{13} h - \frac{6132}{325} s + \frac{9}{130} u_x, \tag{A.16}$$

with

$$s = \omega \left(\frac{2}{3} h_{xx} + \frac{1}{48} f_{xx} \right). \tag{A.17}$$

Fourier transformation of the above equations yields

$$\hat{h}_t = -\left(k^2 + \frac{5}{2} \right) \hat{h} - \frac{5}{64} \hat{f} + \frac{15}{8} \hat{s} + \frac{5}{448} \mathrm{i}\, k\, \hat{u}, \tag{A.18}$$

$$\hat{f}_t = -\left(k^2 + \frac{3059}{130} \right) \hat{f} - \frac{112}{13} \hat{h} - \frac{6132}{325} \hat{s} + \frac{9}{130} \mathrm{i}\, k\, \hat{u}, \tag{A.19}$$

where

$$\hat{s} = -\omega\, k^2 \left(\frac{2}{3} \hat{h} + \frac{1}{48} \hat{f} \right)$$

and

$$\mathrm{i}\, k\, \hat{u} = M\, R \left(60\, \hat{h} + \frac{27}{8} \hat{f} - \frac{1}{5} \hat{s} \right) \text{ with } M = \frac{k^2}{k^4 + 24\, k^2 + 504},$$

with the solution of A.18–A.19

$$\hat{h}(k,t) = K_1\, a_1\, \exp(\sigma_1\, t) + K_2\, a_2\, \exp(\sigma_2\, t), \tag{A.20}$$

$$\hat{f}(k,t) = K_1\, \exp(\sigma_1\, t) + K_2\, \exp(\sigma_2\, t), \tag{A.21}$$

where K_1 and K_2 are constants and

$$a_1 = \frac{1}{2D} \left(A - C + \sqrt{(A-C)^2 + 4DB} \right), \tag{A.22}$$

$$a_2 = \frac{1}{2D} \left(A - C - \sqrt{(A-C)^2 + 4DB} \right), \tag{A.23}$$

$$\sigma_1 = \frac{1}{2} \left(A + C + \sqrt{(A-C)^2 + 4DB} \right), \tag{A.24}$$

$$\sigma_2 = \frac{1}{2} \left(A + C - \sqrt{(A-C)^2 + 4DB} \right), \tag{A.25}$$

with

$$A(k^2,\omega) = -k^2 - \frac{5}{2} + \mathrm{R}\frac{5}{448}\left(60 + \frac{2}{15}\omega k^2\right) M - \frac{5}{4}\omega k^2, \tag{A.26}$$

$$B(k^2,\omega) = \mathrm{R}\frac{5}{448}\left(\frac{27}{8} + \frac{1}{240}\omega k^2\right) M - \frac{5}{64} - \frac{5}{128}\omega k^2, \tag{A.27}$$

$$C(k^2,\omega) = -k^2 - \frac{3059}{130} + \mathrm{R}\frac{9}{130}\left(\frac{27}{8} + \frac{1}{240}\omega k^2\right) M + \frac{511}{1300}\omega k^2, \tag{A.28}$$

$$D(k^2,\omega) = \mathrm{R}\frac{9}{130}\left(60 + \frac{2}{15}\omega k^2\right) M - \frac{112}{13} + \frac{4088}{325}\omega k^2. \tag{A.29}$$

From this we calculate from the dominant growth rate σ_1, by solving

$$\sigma_1 = 0 \qquad \text{and} \qquad \frac{\partial \sigma_1}{\partial R} = 0 \tag{A.30}$$

the critical Rayleigh number $Ra_c = 1350$ together with the critical wavenumber $k_c = 2.52$.

Acknowledgments

The authors thank Andrea Bertozzi for many fruitful discussions. They would also like to thank one of the anonymous referees for some very helpful comments. AM greatly appreciates the support from the DFG Heisenberg fellowship.

References

[1] Lord Rayleigh 1916 On convection currents in a horizontal layer of fluid, when the higher temperature is on the under side *Phil. Mag.* **32** 529–46
[2] Bénard H 1901 Les tourbillons cellulaires dans une nappe liquide transportant de la chaleur par convection en régime permanent *Ann. Chim. Phys.* **23** 62–144
[3] Busse F H 1967 The stability of finite amplitude cellular convection and its relation to an extremum principle *J. Fluid Mech.* **30** 625–649
[4] Clever R M and Busse F H 1974 Transition to time-dependent convection *J. Fluid Mech.* **65** 625–45
[5] Cross M C and Hohenberg P C 1993 Pattern formation outside of equilibrium *Rev. Mod. Phys.* **65** 851–1112
[6] Bodenschatz E, Pesch W and Ahlers G 2000 Recent developments in Rayleigh–Bénard convection *Ann. Rev. Fluid Mech.* **32** 709–78
[7] Manneville P 2006 *Rayleigh–Bénard Convection Thirty Years of Experimental, Theoretical, and Modeling Work* (*Springer Tracts in Modern Physics* vol 207) (Berlin: Springer) pp 41–65
[8] Ahlers G and Behringer R P 1978 Evolution of turbulence from the Rayleigh–Bénard instability *Phys. Rev. Lett.* **40** 712–16
[9] Greenside H S, Cross M C and Coughran W M Jr 1988 Mean flows and the onset of chaos in large-cell convection *Phys. Rev. Lett.* **60** 2269–72
[10] Morris S W, Bodenschatz E, Cannell D S and Ahlers G 1993 Spiral defect chaos in large aspect ratio Rayleigh–Bénard convection *Phys. Rev. Lett.* **71** 2026–9
[11] Assenheimer M and Steinberg V 1993 Rayleigh–Bénard convection near the gas–liquid critical point *Phys. Rev. Lett.* **70** 3888–91
[12] Decker W, Pesch W and Weber A 1994 Spiral defect chaos in Rayleigh–Bénard convection *Phys. Rev. Lett.* **73** 648–51
[13] Pesch W 1996 Complex spatiotemporal convection patterns *Chaos* **6** 348–57
[14] Xi H, Gunton J D and Vinals J 1993 Spiral defect chaos in a model of Rayleigh–Bénard convection *Phys. Rev. Lett.* **71** 2030–3
[15] Tu Y and Cross M C 1996 Defect dynamics for spiral chaos in Rayleigh–Bénard convection *Phys. Rev. Lett.* **75** 834–37
[16] Bestehorn M, Fantz M and Haken H 1992 Spiral patterns in thermal convection *Zeitschrift für Physik B* **88** 93–4

[17] Schmitz R, Pesch W and Zimmermann W 2002 Spiral-defect chaos Swift–Hohenberg model versus Boussinesq equations *Phys. Rev.* E **65** 037302–1
[18] Müller G 1988 Convection and inhomogeneities in crystal growth from the melt *Crystals Growth, Properties, and Applications* ed H C Freyhardt *et al* (Berlin: Springer)
[19] Tang J and Bau H H 1993 Stabilization of the no-motion state in Rayleigh–Bénard convection through the use of feedback control *Phys. Rev. Lett.* **70** 1795–8
[20] Tang J and Bau H H 1993 Feedback control stabilization of the no-motion state in a horizontal, porous layer heated from below *J. Fluid Mech.* **257** 485–505
[21] Tang J and Bau H H 1998 Experiments on the stabilization of the no-motion state of a fluid layer heated from below and cooled from above *J. Fluid Mech.* **363** 153–71
[22] Howle L E 1997 Control of Rayleigh–Bénard convection in a small-aspect-ratio container *Int. J. Heat Mass Trans.* **40** 817–22
[23] Howle L E 1997 Active control of Rayleigh–Bénard convection *Phys. Fluids* **9** 1861–3
[24] Howle L E 2000 The effect of boundary properties on controlled Rayleigh–Bénard convection *J. Fluid Mech.* **411** 39–58
[25] Or A C, Cortelezzi L and Speyer J L 2001 Robust feedback control of Rayleigh–Bénard convection *J. Fluid Mech.* **437** 175–202
[26] Or A C and Speyer J L 2003 Active suppression of finite-amplitude Rayleigh–Bénard convection *J. Fluid Mech.* **483** 111–28
[27] Or A C and Speyer J L 2005 Gain-scheduled controller for the suppression of convection at high Rayleigh number *Phys. Rev.* E **71** 046302
[28] Remillieux M C, Zhao H and Bau H H 2007 Suppression of Rayleigh–Bénard convection with proportional-derivative controller *Phys. Fluids* **19** 017102
[29] Orszag S A and Thess A 1995 Surface-tension-driven Bénard convection at infinite Prandtl number *J. Fluid Mech.* **283** 201–29
[30] Howle L E 1997 Linear stability analysis of controlled Rayleigh–Bénard convection using shadowgraphic measurement *Phys. Fluids* **9** 3111–3113
[31] Wagner B A, Bertozzi A L and Howle L E 2003 Positive feedback control of Rayleigh–Bénard convection *Discrete Cont. Dyn.* B **3** 619–42
[32] Plaut E and Pesch W 1999 Extended weakly nonlinear theory of planar nematic convection *Phys. Rev.* E **59** 1747–69
[33] Manneville P 1983 A two-dimensional model for three-dimensional convective patterns in wide containers *J. Physique* **4** 759–65
[34] Lagha M and Manneville P 2007 Modeling transitional plane Couette flow *Eur. Phys. J.* B **58** 433–47
[35] Ruyer-Quil C and Manneville P 2002 Further accuracy and convergence results on the modeling of flows down inclined planes by weighted-residual approximations *Phy. Fluids* **14** 170–83
[36] Todd F Dupont and Hosoi A E 1998 Some reduced-dimension models based on numerical methods *Modelling and Computation for Applications in Mathematics, Science and Engineering* (Oxford: Oxford University Press) pp 59–80
[37] Skalický T 1996 Laspack reference manual Version 1.12.3, Dresden University of Technology, Institute for Fluid Mechanics
[38] Quateroni A and Canuto C 1982 Approximation results for orthogonal polynomials in Sobolev spaces *Math. Comp.* **38** 67–86